Inorganica Chimica Acta 394 (2013) 715–722

Contents lists available at SciVerse ScienceDirect

Inorganica Chimica Acta

journal homepage: www.elsevier.com/locate/ica

Ligand-controlled assembly of cobalt(II) metal–organic complexes from different semirigid bis(imidazole) derivatives and aromatic monocarboxylates: Electrochemical behaviors and fluorescent properties

Lian-Li Liu, Jing-Jing Huang, Xiu-Li Wang *, Guo-Cheng Liu, Song Yang, Hong-Yan Lin

Department of Chemistry, Bohai University, Liaoning Province Silicon Materials Engineering Technology Research Centre, Jinzhou 121000, PR China

ARTICLE INFO

Article history:
Received 19 June 2012
Received in revised form 24 September 2012
Accepted 27 September 2012
Available online 12 October 2012

Keywords:
Conformation of ligands
Crystal structure
Semirigid bis(imidazole) derivative
Electrochemical behaviors
Fluorescent properties

ABSTRACT

To explore the influence of the conformation and substitute group of organic ligands on constructing coordination polymers, we synthesized four Co(II) metal–organic complexes, namely, $[Co(bix)(BBA)_2]_2$ (**1**), $[Co(bix)(DNBA)_2]$ (**2**), $[Co(dmpbbbm)(BBA)_2]$ (**3**) and [Co(dmpbbbm)(DNBA)(Cl)] (**4**) (bix = 1,4-bis(imidazol-1-ylmethyl)benzene, dmpbbbm = 1,4-bis(5,6-dimethylbenzimidazol-1-ylmethyl)benzene, HBBA = 4-bromobenzoic acid, HDNBA = 3,5-dinitrobenzoic acid) under hydrothermal conditions. Complex **1** is a dinuclear cluster and is finally extended into a one-dimensional (1D) supramolecular chain though H-bonding interactions. Complex **2** shows 1D right-handed helical chains. Complex **3** possesses *meso*-helical chains with left- and right-handed helix, which is further extended into a two-dimensional (2D) supramolecular wave-like network through π–π stacking interactions. Complex **4** exhibits a *meso*-helical chain with left- and right-handed helical loops in one single strand, which is ultimately packed into a three-dimensional (3D) supramolecular framework through π–π stacking interactions. In addition, the thermal stability, the fluorescent properties and the electrochemical behaviors of the title complexes at room temperature have been investigated.

1. Introduction

As the foundation of the genetic code, helical structures have received much attention in coordination chemistry not only for their ubiquitous appearance in nature, but also for their promising applications in multidisciplinary areas, such as biomimetic chemistry and structural biology [1–6]. Sometimes, such helical structures were considered as the primary structures, which can be further organized to supramolecular structures by coordination or/and hydrogen bonds or other weaker supramolecular interactions, such as π–π stacking interactions [7–9]. It is important to rationally design the organic ligands and to choose metal salts with suitable coordination geometry in the self-assembly synthesis of such species [10,11]. However, the structure of coordination polymers is influenced by substitute group and conformation of organic ligands, molar ratio of reactants, and pH value of the solution, etc., which makes the controllable preparation of the target metal organic complexes still be a great challenge [12–14].

With this understanding, we select two semirigid ligands 1,4-bis(imidazol-1-ylmethyl)benzene (bix) and 1,4-bis(5,6-dimethylbenzimidazol-1-ylmethyl)benzene (dmpbbbm) as N-heterocyclic ligands. In our previous research, we usually use flexible double imidazole derivative ligands [15–18]. Comparing with those ligands, dmpbbbm or bix not only possesses two freely rotating imidazole or 5,6-dimethylbenzimidazole arms, but also has a rigid spacer of phenyl ring, which may generate two flexures and favor the formation of helical motifs [19]. In addition, the aromatic ring system may provide potential supramolecular recognition sites for π–π stacking interactions. The two N-donor ligands were chosen here to investigate the effect of conformations and substituting group of ligand on the structures of complexes. To the best of our knowledge, dmpbbbm ligand used in the complexes has not been reported up to now.

Taking all of the above discussion into account, by introducing two aromatic monocarboxylate coligands, that is, 4-bromobenzoic acid (HBBA) and 3,5-dinitrobenzoic acid (HDNBA), four Co(II) coordination polymers with different structures, namely $[Co(bix)(BBA)_2]_2$ (**1**), $[Co(bix)(DNBA)_2]$ (**2**), $[Co(dmpbbbm)(BBA)_2]$ (**3**), and [Co(dmpbbbm)(DNBA)(Cl)] (**4**) have been obtained. The effect of conformations and substituting group of ligands on the ultimate framework have been represented and discussed. Moreover, the thermal stability, photoluminescence properties along with electrochemical properties of **1**–**4** have also been investigated in detail.

* Corresponding author. Tel.: +86 416 3400158.
E-mail address: wangxiuli@bhu.edu.cn (X.-L. Wang).

0020-1693/$ - see front matter © 2012 Elsevier B.V. All rights reserved.
http://dx.doi.org/10.1016/j.ica.2012.09.033

2. Experimental

2.1. Materials and measurements

All chemicals used for synthesis were of reagent grade and used without further purification. The dmpbbbm and bix ligands were prepared according to the literature method [20]. Elemental analyses were performed on a Perkin-Elmer 240CHN analyzer. Thermogravimetric analyses (TGA) were carried out using a Pyris Diamond thermal analyzer. The luminescence spectra were measured on a HITACHI F-4500 Fluorescence Spectrophotometer. The electrochemical properties were performed on a CHI 440 Electrochemical Quartz Crystal Microbalance. A conventional three-electrode cell was used at room temperature. The **1**-, **2**-, **3**- and **4**-CPE were used as working electrodes. An SCE and a platinum wire were used as reference and auxiliary electrodes, respectively.

2.2. Preparation of the complexes **1–4**

2.2.1. $[Co(bix)(BBA)_2]_2$ (**1**)

A mixture of $CoCl_2{\cdot}6H_2O$ (0.0238 g, 0.1 mmol), bix (0.0242 g, 0.1 mmol) and HBBA (0.04 g, 0.2 mmol) was dissolved in 10 mL H_2O. The pH value was adjusted about 7 with 0.1 M NaOH solution. The resulting mixture was sealed in a 25 mL Teflon reactor and then heated at 150 °C for 3 days. After the reactor was cooled to room temperature at a rate of 5 °C h^{-1}, purple block-shaped crystals of **1** were gained, washed with distilled water, and dried in air. For complex **1**, yield: 37% (based on Co). Elemental *Anal.* Calc. for $C_{56}H_{44}Br_4Co_2N_8O_8$: C, 48.23; H, 3.18; N, 8.04. Found: C, 48.17; H, 3.13; N, 8.16%. IR (KBr), ν/cm^{-1}: 3419 w, 3174 s, 3008 m, 1591 s, 1550 s, 1384 s, 1164 m, 771 m, 655 w.

2.2.2. $[Co(bix)(DNBA)_2]$ (**2**)

Similar procedure was used to synthesize the purple block crystals of complex **2**, except that HDNBA (0.042 g, 0.2 mmol) was used instead of HBBA for preparation of **1**. Yield: 54% (based on Co). Elemental *Anal.* Calc. for $C_{28}H_{20}CoN_8O_{12}$: C, 46.74; H, 2.80; N, 15.58. Found: C, 46.59; H, 2.85; N, 15.47%. IR (KBr), ν/cm^{-1}: 3373 w, 3089 m, 1624 s, 1577 m, 1539 s, 1461 m, 1444 w, 1344 s, 1292 w, 1091 m, 792 w, 727 s, 655w.

2.2.3. $[Co(dmpbbbm)(BBA)_2]$ (**3**)

Similar procedure was used to synthesize the purple block crystals of complex **3**, except that dmpbbbm (0.039 g, 0.1 mmol) was used instead of bix for preparation of **1**. Yield: 42% (based on Co). Elemental *Anal.* Calc. for $C_{40}H_{34}Br_2CoN_4O_4$: C, 56.29; H, 4.02; N, 6.56. Found: C, 56.42; H, 3.87; N, 6.71%. IR (KBr), ν/cm^{-1}: 3423 w, 3168 s, 3012 m, 1589 s, 1546 m, 1400 s, 1275 m, 1194 w, 857 w, 736 m.

2.2.4. $[Co(dmpbbbm)(DNBA)(Cl)]$ (**4**)

The same synthetic method as that for **1** was used except that bix was replaced by dmpbbbm (0.039 g, 0.1 mmol) and HBBA was replaced by HDNBA (0.042 g, 0.2 mmol). Blue block-shaped crystals of **4** were gained. Yield: 40% (based on Co). Elemental *Anal.* Calc. For $C_{33}H_{29}ClCoN_6O_6$: C, 56.62; H, 4.18; N, 12.01. Found: C, 56.38; H, 4.24; N, 12.27%. IR (KBr), ν/cm^{-1}: 3427 w, 3109 m, 1624 s, 1541 m, 1382 m, 1344 s, 1278 m, 1218 m, 1068 w, 858 w, 727 s.

2.3. Preparation of the **1**-, **2**-, **3**- and **4**-CPEs

Complex **1**-modified carbon-paste electrode (**1**-CPE) was fabricated according to the literature method [21]: 0.04 g complex **1** and 0.6 g graphite powder were mixed and ground together by agate mortar and pestle for approximately 40 min to achieve an even mixture, and then 0.2 mL paraffin oil was added and stirred with a glass rod. The homogenized mixture was pack into a glass tube (3 mm inner diameter) to a length of 6 mm. The electrical contact was established with the copper stick and the surface of the **1**-CPE was wiped with weighing paper [22]. A similar procedure was used for the preparation of **2**-CPE, **3**-CPE and **4**-CPE and bare CPE without any complexes.

2.4. X-ray crystallographic study

The diffraction data of the four complexes were collected on a Bruker Smart 1000 CCD area detector diffractometer with Mo Kα radiation (λ = 0.71073 Å for **1**–**4**) by using an ω–2θ scan mode. The crystal structures were solved by the direct method and refined with a full-matrix least-squares technique based on F^2 with the SHELXL-97 software package [23]. All the non-hydrogen atoms were refined with anisotropic thermal parameters on F^2. The hydrogen atoms of ligands were placed in geometrically idealized positions and refined isotropically with thermal factors. In the complex **4**, the O1, O2, C1, O5, O6, N5 of the DNBA anions were refined as disordered atoms. Distances restraints (DFIX) were applied in the unreasonable C32 N6 O4 O7 positions of complex **4**. The detailed crystallographic data and structure processing parameters for complexes **1**–**4** are listed in Table 1. Selected bond lengths and angles of complexes **1**–**4** are summarized in Table S1 of the Supporting Information.

3. Results and discussion

3.1. Description of crystal structures

3.1.1. $[Co(bix)(BBA)_2]_2$ (**1**)

The X-ray crystallographic study shows that complex **1** crystallizes in the asymmetrical triclinic space group $P\bar{1}$, and exhibits a dinuclear structure. As shown in Fig. 1(a), there are one crystallographically independent Co(II) atom, one bix ligand and two BBA ligands in the asymmetric unit of **1**. The Co(II) atom is coordinated by two oxygen atoms (O1, O3) from two BBA ligands and two nitrogen atoms (N1, N4A) from two bix ligands, showing a distorted tetrahedral geometry. The Co–O bond distances are 1.958(3) and 1.996(3) Å, while the Co–N bond length are between 2.016(3) and 2.031(4) Å. The bond angles of O–Co–O are 110.88(15)°, while the bond angles of N–Co–N are 114.90(16)°. The bond angles of N–Co–O are in the range of 95.58(15)–116.34(15)°.

The carboxylic groups of BBA ligands coordinate to Co(II) atoms, adopting a monodentate coordination mode. The bix ligand acts as bidentate ligand to bridge two Co(II) atoms, which exhibits *cis*-configuration with a $N_{donor}\cdots N{-}C_{sp3}\cdots C_{sp3}$ torsion angle of 81.82°. The dihedral angle between the pairs of imidazole rings is 55.22°. Two bix ligands connect neighboring Co(II) atoms to form a dinuclear cluster with the distance of 10.820 Å between Co(II) atoms. In addition, the structure is further extended by C–H···O hydrogen bonding interactions between the carboxylic oxygen atoms from BBA anions and the C–H from the adjacent imidazole rings [C(12)–H(12A)···O(1): 3.271 Å] to afford a one-dimensional (1D) supramolecular chain. Zheng and co-workers have obtained a similar ring in $\{[Zn(L)(bix)]_3(H_2O)(DMF)_2\}_n$ (L = 4,4′-(hexafluoroisopropylidene)bis(benzoic acid)) complex [24]. The bix ligand adopts similar *cis*-conformation with the dihedral angles between imidazole and phenyl are 71.791(4)° and 86.333(4)°, which is a little different from 75.18° and 84.68° in **1**.

3.1.2. $[Co(bix)(DNBA)_2]$ (**2**)

Single crystal X-ray diffraction analysis reveals that **2** crystallizes in the monoclinic space group *C*2, exhibits a 1D right-handed

Table 1
Crystal data and structure refinement details for complexes **1**–**4**.

Complex	1	2	3	4
Formula	$C_{56}H_{44}Br_4Co_2N_8O_8$	$C_{28}H_{20}CoN_8O_{12}$	$C_{40}H_{34}Br_2CoN_4O_4$	$C_{33}H_{29}ClCoN_6O_6O_6$
Formula wt.	1394.45	719.45	853.44	700.00
Crystal system	triclinic	monoclinic	monoclinic	monoclinic
Space group	$P\bar{1}$	$C2$	$C2/c$	$C2/c$
a (Å)	10.076(2)	22.432(4)	25.0246(15)	19.1278(11)
b (Å)	12.750(3)	6.2562(12)	6.2508(4)	16.8327(10)
c (Å)	13.189(3)	11.100(2)	22.7773(13)	21.3003(12)
α (°)	64.037(3)	90	90	90
β (°)	80.602(3)	99.851(3)	95.951(2)	99.3350(10)
γ (°)	68.594(3)	90	90	90
V (Å^{-3})	1418.4(6)	1534.8(5)	3543.7(4)	6767.3(7)
Z	1	2	4	8
D (g cm^{-3})	1.633	1.557	1.600	1.374
μ (mm^{-1})	3.462	0.637	2.788	0.638
$F(000)$	694.0	734	1724	2888
θ_{max} (°)	24.99	26.47	27.70	28.33
Total data collected	9622	4461	28 212	30 123
Unique data reflections	4999	1736	4152	8431
R_{int}	0.0214	0.0198	0.0252	0.0395
R_1[a] [$I>2\sigma(I)$]	0.0559	0.0688	0.0400	0.0591
wR_2[b] (all data)	0.1839	0.2012	0.1086	0.1952
GOF	1.003	1.008	1.022	1.047
$\Delta\rho_{max}$ (e Å^{-3})	1.521	0.557	1.324	1.112
$\Delta\rho_{min}$ (e Å^{-3})	−1.514	−0.308	−1.140	−0.452

[a] $R_1 = \Sigma(||F_o| - |F_c||)/\Sigma|F_o|$.
[b] $wR_2 = [w(|F_o|^2 - |F_c|^2)^2/(w|F_o|^2)^2]^{1/2}$.

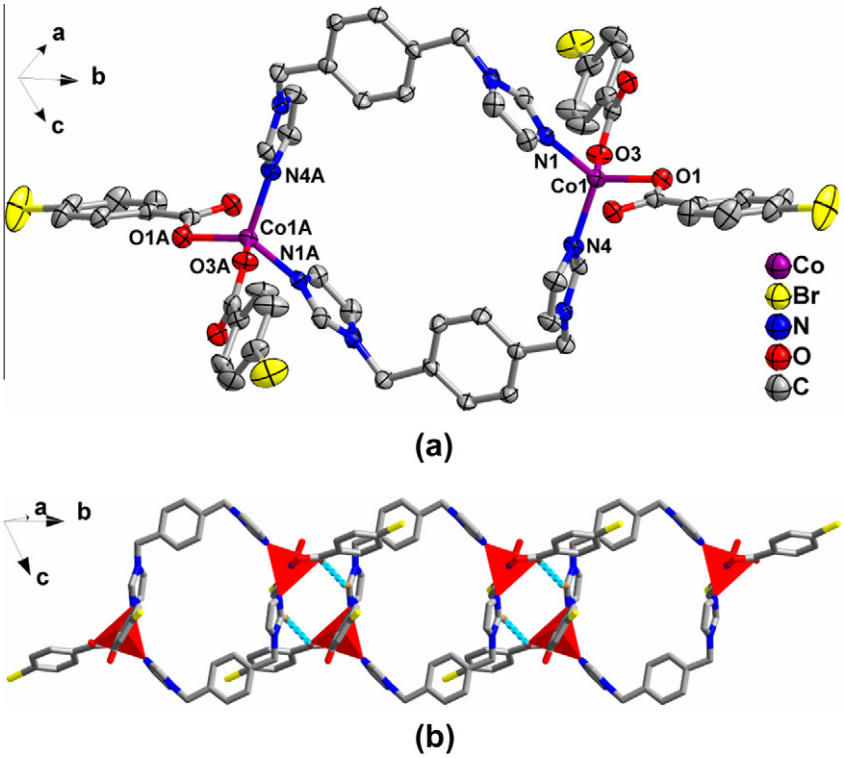

Fig. 1. (a) The coordination environment of Co(II) in complex **1**, showing a distorted tetrahedral geometry. The hydrogen atoms were omitted for clarity. (b) The dinuclear unit is extended into 1D supramolecular structure by H-bonding interactions.

helical chain. As illustrated in Fig. 2(a), the asymmetric unit of **2** possesses one Co(II) atom, one bix ligand and two symmetry-related DNBA anions. Each Co(II) atom is coordinated by two nitrogen atoms (N1, N1A) from two bix ligands and four oxygen atoms (O1, O2, O1A, O2A) from two carboxylic groups of different DNBA anions, showing an octahedral geometry. The lengths of Co–O and Co–N are 2.169(7)–2.295(8) Å, and 2.034(6) Å, respectively. The bond angles of N–Co–O are in the range of 90.1(3)–142.4(2)°, while the bond angles of O–Co–O are from 55.3(3)° to 165.5(5)°. The bond angle of N–Co–N is 106.4(3)°.

In complex **2**, the deprotonated carboxylic groups of DNBA anions adopt chelating coordination mode to coordinate with Co(II) atoms. Semirigid bix ligand adopts *cis*-conformation with a $N_{donor}\cdots N{-}C_{sp3}\cdots C_{sp3}$ torsion angle of 82.80°, which connect adjacent

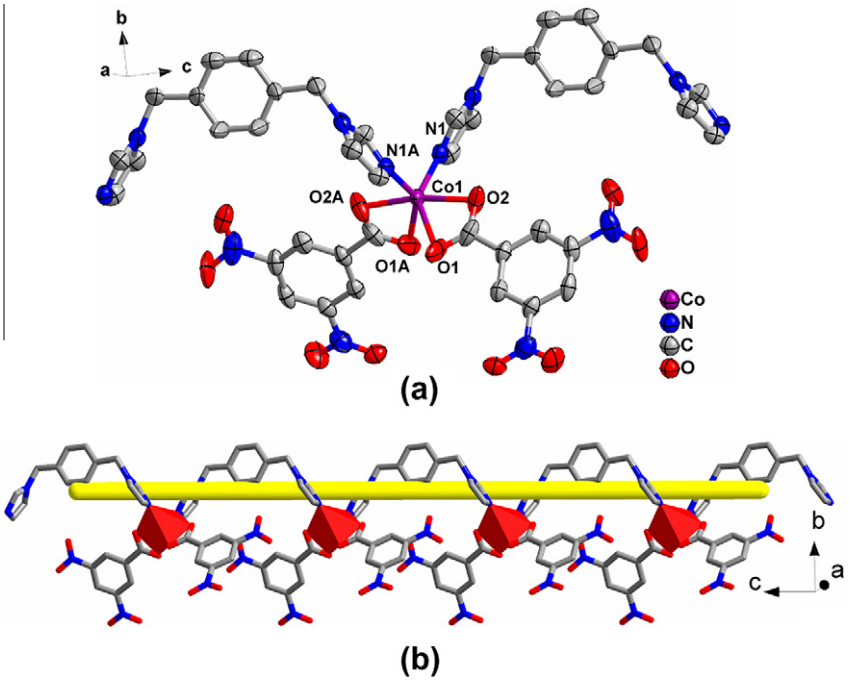

Fig. 2. (a) The coordination environment of Co(II) in complex **2**, showing a distorted octahedral geometry. The hydrogen atoms were omitted for clarity. (b) View of the 1D right-handed helical chain of complex **2**.

Co(II) atoms to form a 1D right-handed helical chain with a period of 11.10 Å. The dihedral angle between the pairs of imidazole rings is 63.97°. The bix ligand was also employed by Ma and Yang's group in synthesizing [Cd(L)(bix)] (L = (R)-2-(4′-(4″-carboxybenzyloxy)phenoxy)propanoic acid). However, the bix ligand displayed *trans*-conformation to form a left-handed helical chain with a period of 21.8367(7) Å [25].

3.1.3. [Co(dmpbbbm)(BBA)$_2$] (**3**)

Single crystal X-ray diffraction analysis shows that **3** crystallizes in the monoclinic space group *C*2/*c*, and shows 1D *meso*-helical chains. As depicted in Fig. 3(a), the asymmetric unit of **3** consists of one Co(II) atom, one dmpbbbm ligand and two BBA ligands. The Co(II) atom shows a distorted octahedral geometry, which is six-coordinated by four oxygen atoms (O1, O2, O1A, O2A) from two carboxylate groups and two nitrogen atoms (N1, N1A) from two dmpbbbm ligands. The Co–O bond lengths vary from 2.174(2) to 2.235(3) Å, while the Co–N bond length is 2.070(2) Å. The bond angles of N–Co–O are in the range of 87.81(9)–141.70(9)°, while the bond angles of O–Co–O are from 58.50(9)° to 172.70(16)°. The bond angle of N–Co–N is 105.16(12)°.

In complex **3**, the BBA ligand adopts a chelating coordination mode. The semirigid dmpbbbm ligands connect adjacent Co(II) atoms to form a 1D *meso*-helical chain with left- and right-handed loops in one single strand along the *a*-axis (Fig. 3(b)). The helical pitch is 22.777 Å corresponding to the length of the *a*-axis, and the Co···Co separation across the dmpbbbm bridge is 13.480 Å. The similar left- and right-handed helical chain in one single strand was obtained by Puddephatt and co-workers based on the semirigid *N*,*N*-bis(pyridin-3-yl)-1,3-benzenedicarboxamide ligand [26]. The dmpbbbm adopts *trans*-conformation with the $N_{donor}\cdots N{-}C_{sp3}\cdots C_{sp3}$ torsion angle of 71.03°, which displays two flexures with opposite direction. The extension of the structure into a two-dimensional (2D) wave-like network is accomplished by π–π stacking interactions between the aromatic rings from BBA anions and dmpbbbm ligands with the face-to-face distance of 3.874 Å.

3.1.4. [Co(dmpbbbm)(DNBA)(Cl)] (**4**)

The single crystal X-ray diffraction analysis reveals that **4** also exhibits a 1D *meso*-helical chain and crystallizes in the monoclinic system, space group *C*2/*c*. The asymmetric unit of **4** contains a tetrahedral Co(II) atom (Fig. 4), which is provided by two nitrogen atoms (N1, N3) from two dmpbbbm ligands and one oxygen atom (O1) from the carboxylic group of DNBA anion and one chlorine anion at the axial sites. The lengths of Co–O, Co–N and Co–Cl are 1.934(9), 2.003(3)–2.007(2) and 2.2288(10) Å, respectively. The bond angles of N–Co–O are from 112.0(3)° to 116.8(3)°, while the bond angle of N–Co–N is 101.76(10)°.

It should be noted that the dmpbbbm ligands show two kinds of coordination conformations in complex **4**. One takes a twisted *cis*-conformation with a $N_{donor}\cdots N{-}C_{sp3}\cdots C_{sp3}$ torsion angle of 94.39°, which bridges two adjacent Co(II) atoms with Co···Co distance of 12.03 Å. The other shows *trans*-conformation with a $N_{donor}\cdots N{-}C_{sp3}\cdots C_{sp3}$ torsion angle of 76.10°, which bridges two adjacent Co(II) atoms with Co···Co distance of 13.45 Å. Hinging at metal ions, the pitch of the *meso*-helix is 15.823 Å, corresponding to the length of *a*-axis. The dihedral angle between the pairs of benzimidazole rings in the *cis*-conformation ligand is 44.6° in contrast to that in the *tran*-conformation ligand of 180°. A similar 1D *meso*-helical chain was obtained in complex $\{[Zn(bmb)(2,6\text{-}pydc)]_3\cdot 2H_2O\}_n$ (bmb = 1,4-bis(2-methylbenzimidazol-1-ylmethyl)benzene, 2,6-H_2pydc = 2,6-pyridinedicarboxylic acid) by Hou and co-workers [1]. The N-donor ligand only adopts *trans*-conformation with a $N_{donor}\cdots N{-}C_{sp3}\cdots C_{sp3}$ torsion angle of 80.221°. Besides that, the helical pitch is 18.535 Å in complex $\{[Zn(bmb)(2,6\text{-}pydc)]_3\cdot 2H_2O\}_n$, which is longer than that in **4**. The deprotonated carboxylic group of DNBA anion adopts monodentate mode to coordinate with Co(II) atom. The dmpbbbm bridging neighboring Co(II) atoms afford a fascinating 1D *meso*-helical chain with left- and right-handed helical loops in one single strand (Fig. 5(a)). Viewing from the *c*-axis, the projection of the helical chain on the *ab* plane look likes "8" shape (Fig. 5(b)). Moreover, the discrete *meso*-helical chains are extended to three-dimensional (3D) supramolecular network (Fig. 5(c)) by π–π stacking interactions between the aromatic rings

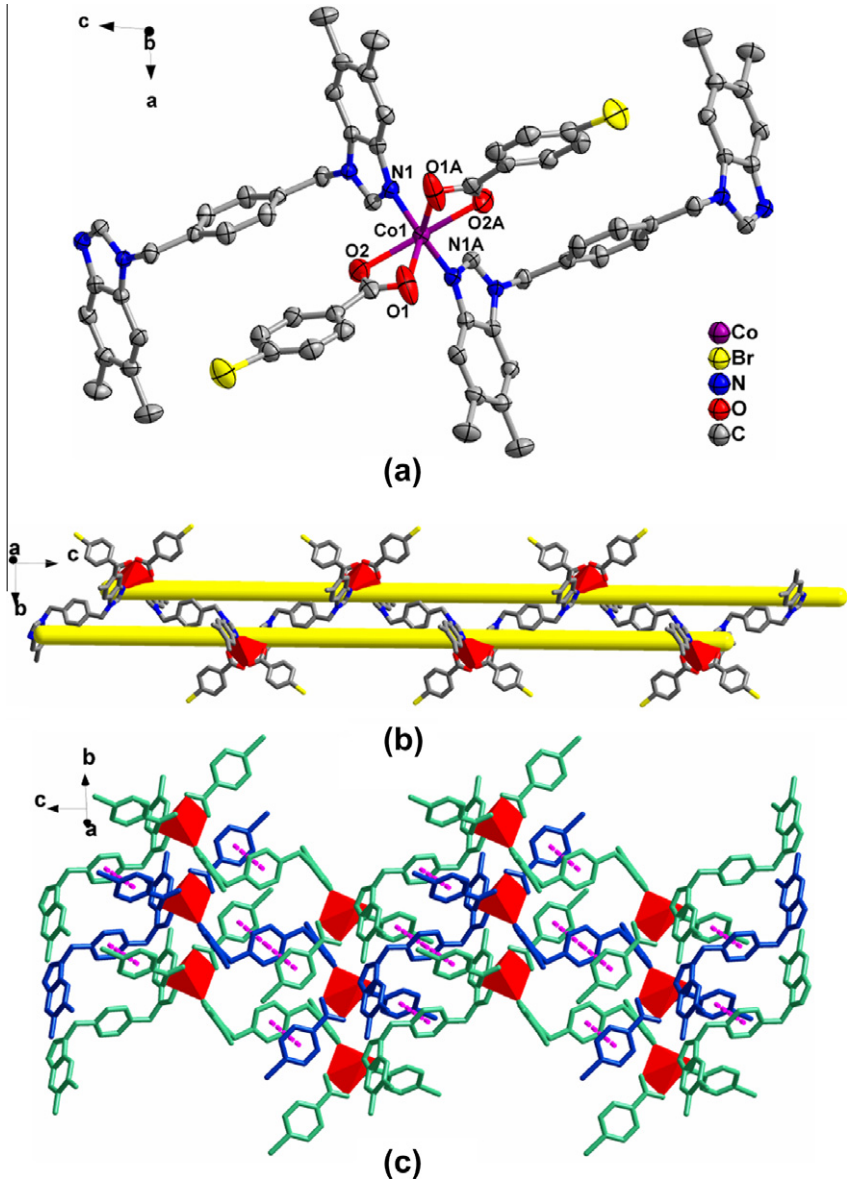

Fig. 3. (a) The coordination environment of Co(II) in complex **3**, showing a octahedral geometry. The hydrogen atoms were omitted for clarity. (b) View of the 1D left- and right-handed helical chain of complex **3**. (c) The 1D chains are connected to 2D supramolecular network by π–π stacking interactions.

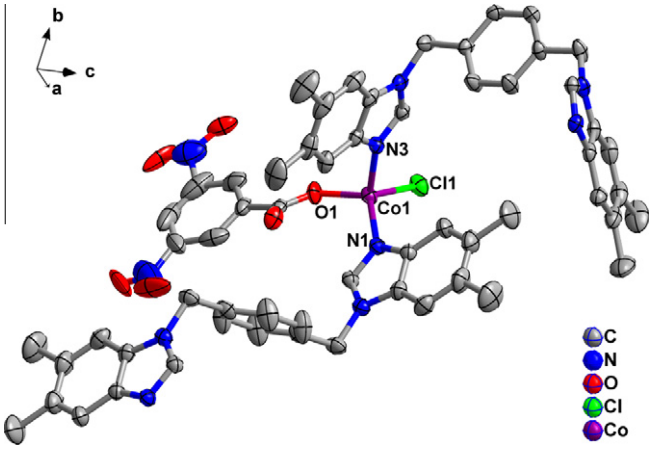

Fig. 4. The coordination environment of Co(II) in complex **4**, showing a distorted tetrahedral geometry. The hydrogen atoms were omitted for clarity.

from DNBA anions and 5,6-dimethylbenzimidazole with the face-to-face distance of 3.817 Å.

3.2. Effect of the conformation and substitute groups of ligands on complexes *1–4*

The conformation and flexibility of ligands are considered to be the important factors for the formation of helical features. Semi-rigid ligands (bix and dmpbbbm), contain a rigid spacer of phenyl ring and two freely twisting imidazole or 5,6-dimethylbenzimidazole arms, respectively. The ligands are principally divided into two types: the same direction (*cis*-) and the opposite direction (*trans*-) on the basis of the difference in the relative orientations of two imidazole or 5,6-dimethylbenzimidazole rings in the ligands [27]. The two conformations can transform to each other to suit the coordination environment of the metal cations. The reason may be that the flexible $-CH_2-$ group makes the two terminal groups significantly deviate from co-planarity with a potential

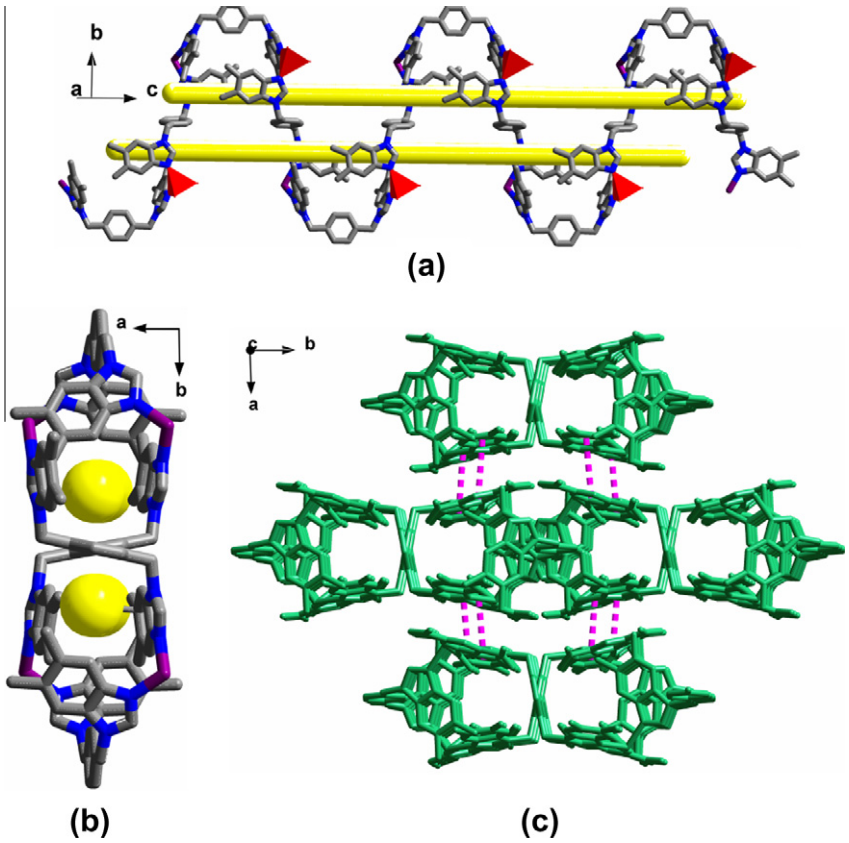

Fig. 5. (a) View of the 1D *meso*-helical chain of **4**. (b) The projection of helical chain look likes "8" along *c* axis. (c) The *meso*-helical chains are interconnected to form 3D supramolecular framework by π–π stacking interactions.

tendency to form versatile *cis*- and *trans*-conformations when bix or dmpbbbm coordinates with metal cations [28,29]. From the structural descriptions above, it shows *cis*-conformation in **1** and **2**, and the $N_{donor}\cdots N{-}C_{sp3}\cdots C_{sp3}$ torsions angles are 81.75° and 82.80°, respectively. The Co···Co distances are 10.82 and 11.10 Å, respectively. In **3**, the dmpbbbm ligand adopt *trans*-conformation with $N_{donor}\cdots N{-}C_{sp3}\cdots C_{sp3}$ torsion angle of 71.03° and the Co···Co distances of 13.48 Å. Compared with the complexes **1**–**3**, complex **4** takes two kinds of conformations, *cis*- and *trans*-conformation, with the $N_{donor}\cdots N{-}C_{sp3}\cdots C_{sp3}$ torsion angles of 94.39° and 76.10°, respectively. The Co···Co distances are 12.03 and 13.446 Å, respectively. As shown in Fig. 6, the Co···Co distances in complexes **3** and **4** are a little longer than those in **1** and **2**, which may be attributed to the steric hindrance of the substituent groups of dmpbbbm. Moreover, the dmpbbbm ligand is easier to form *trans*-conformation than the bix ligand, which is probably due to the steric hindrance of the substituent groups of dmpbbbm increasing the flexures of ligand.

Complexes **1** and **3** exhibit different structures based on the same carboxylic ligand. The bix bridge two adjacent Co(II) atoms to form a dinuclear structure in **1**, while the dmpbbbm act as bidentate ligands to generate a 1D left- and right-handed helical chain in **3**. Complexes **2** and **4** based on DNBA anion ligand show different structures, too. In **2**, the bix connect adjacent Co(II) atoms to form a 1D right-handed chain, however, the dmpbbbm ligands bridging neighboring Co(II) atoms afford a 1D *meso*-helical chain in **4**. All of these may be ascribed to the different N-heterocyclic ligands. The steric hindrance of the substituent groups of dmpbbbm ligand ultimately results in the different structures. In addition, it has been demonstrated that the structural diversities of the complexes are undoubtedly related to the secondary auxiliary ligand [30]. In complex **1**, BBA ligands act as hydrogen bonding acceptors which make the dinuclear structure extend into a 1D chain. In **3**, BBA ligands play an important role in constructing 2D supramolecular wave-like network by π–π stacking interactions. When DNBA carboxylic ligand with two nitro groups is introduced into the synthetic procedure, a 1D right-handed helical chain **2** decorated with DNBA at one side is constructed and a 3D supramolecular network in **4** was obtained by π–π stacking interactions. So, the introduction of monocarboxylate

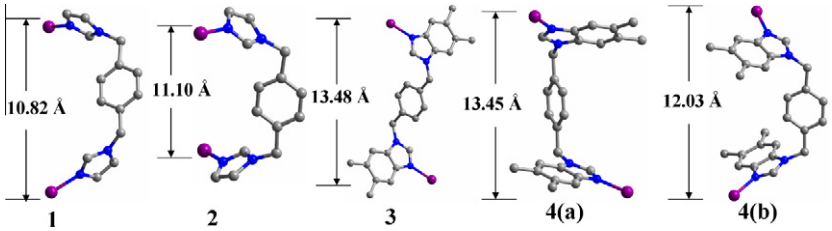

Fig. 6. The conformations of bix and dmpbbbm in complexes **1**–**4**.

coligands may effectively adjust the structure features and build much more various structures.

3.3. Properties

3.3.1. IR spectroscopy

The main features of IR spectra for complexes **1**–**4** concern the carboxylate groups of BBA or DNBA and the N-heterocyclic rings of dmpbbbm or bix ligand. No strong absorption peaks around 1700 cm^{-1} for –COOH implies that carboxyl groups of organic moieties in the title complexes are completely deprotonated [31,32]. The peaks at 1591, 1384 cm^{-1} for **1** (1624, 1577 cm^{-1} for **2**; 1589, 1400 cm^{-1} for **3**; 1624, 1382 cm^{-1} for **4**) can be considered as vibrations of carboxylate groups. The peaks at 1550, 1164, 771 cm^{-1} for **1** (1461, 1091, 727 cm^{-1} for **2**; 1546, 1275, 736 cm^{-1} for **3**; 1278, 1218, 727 cm^{-1} for **4**) can be attributed to ν_{C-N} of N-heterocyclic rings of bix or dmpbbbm ligands. The presence of bands at 3174, 3008 cm^{-1} for **1** (3089 cm^{-1} for **2**; 3168, 3012 cm^{-1} for **3**; 3109 cm^{-1} for **4**) can be considered as ν_{C-C} of $-CH_3$ or $-CH_2-$ of bix and dmpbbbm ligands. The peaks at 1539 and 1344 cm^{-1} for **2** (1541 and 1344 cm^{-1} for **4**) can be attributed to the $\nu(-NO_2)$ (see Figs. S1–S4).

3.3.2. Thermal stability analysis

To characterize the complexes **1**–**4** more fully in terms of thermal stability, their thermal behaviors were investigated by thermogravimetric analysis (TGA). The TG curves of complexes **1**–**4** exhibit only one obvious weight loss step (Fig. 7). The framework of complexes **1** and **2** began to collapse from 290 °C, while the complexes **3** and **4** are more stable up to 340 °C, where the decomposition of the framework starts. Pyrolysis of the residual substance with a series of consecutive weight losses (88.63% for **1**, 88.84% for **2**, 91.86% for **3**, 90.04% for **4**) stops at 680 °C for **1**, 660 °C for **2**, 700 °C for **3** and 720 °C for **4**, which implies the decomposition of organic ligands bix or dmpbbbm and BBA or DNBA (calculated: 89.24% for **1**, 89.58% for **2**, 91.21% for **3**, 89.29% for **4**). The remaining residue weight (10.76% for **1**, 10.42% for **2**, 8.79% for **3**, 10.71% for **4**) is presumed to be CoO (calculated: 10.06% for **1**, 10.97% for **2**, 9.49% for **3**, 10.24% for **4**).

3.3.3. Fluorescence properties of complexes *1*–*4*

Luminescent complexes are attracting more and more attention due to their various potential applications [33,34], such as chemical sensors, white light-emitting diodes (LEDs), and electroluminescent materials (OLEDs) for displays [35,36]. Hence, the solid state photoluminescent properties of complexes **1**–**4**, free bix and dmpbbbm ligands were investigated at room temperature. As illustrated in Fig. 8, complexes **1** and **2** exhibit intense emission bands with a maximum at 415 nm upon excitation at 268 nm and a maximum at 427 nm upon excitation at 260 nm, respectively. The fluorescent emission peaks of **1** and **2** can be probably assigned to the intraligand $\pi^*-\pi$ charge transitions of bix (λ_{em} = 432 nm, λ_{ex} = 340 nm) due to their similar emission peaks. The fluorescent emission peaks can be observed at 446 nm (λ_{ex} = 265 nm) for **3** and 456 nm (λ_{ex} = 275 nm) for **4**, which are different from that of (λ_{em} = 395 nm, λ_{ex} = 320 nm) dmpbbbm ligand. The significant red-shift should be attributed to the metal–ligand coordination interactions. Compared with the complexes **1** and **3**, the significant red-shift in **2** and **4** may be attributed to the coordination interactions of DNBA anions and metal ions [37].

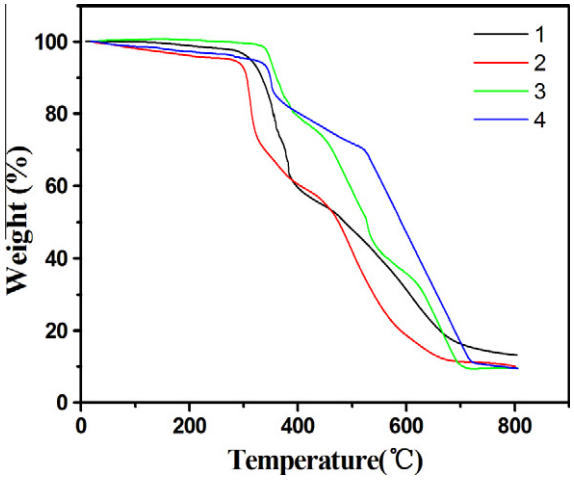

Fig. 7. The TG curves of complexes **1**–**4**.

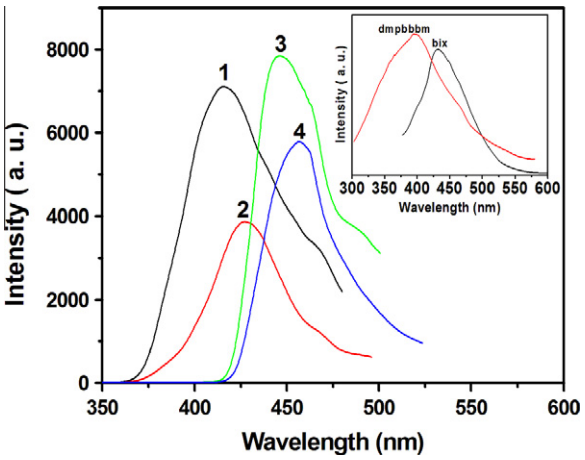

Fig. 8. Emission spectra of two free N-ligands and complexes **1**–**4** in the solid state at room temperature.

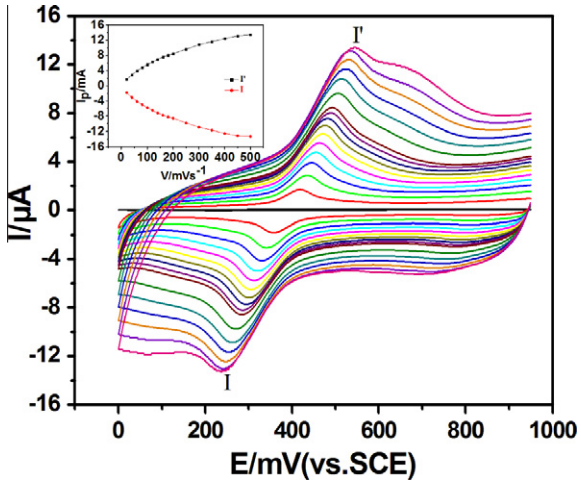

Fig. 9. Cyclic voltammograms of the **2**-CPE in 1 M H_2SO_4 aqueous solution at different scan rates (from inner to outer: the bare CPE, 20, 40, 60, 80, 100, 120, 140, 160, 180, 200, 250, 300, 350, 400, 450, 500 mV s^{-1}). The inset shows the plots of the anodic and cathodic peak currents against scan rates.

3.3.4. Electrochemical properties of complexes *1*–*4*

In order to study the redox properties of the Co(II) complexes, the **1**–**4** bulk-modified carbon paste electrode (**1**-, **2**-, **3**- and **4**-CPE) becomes the optimal choice due to their insolubility in water

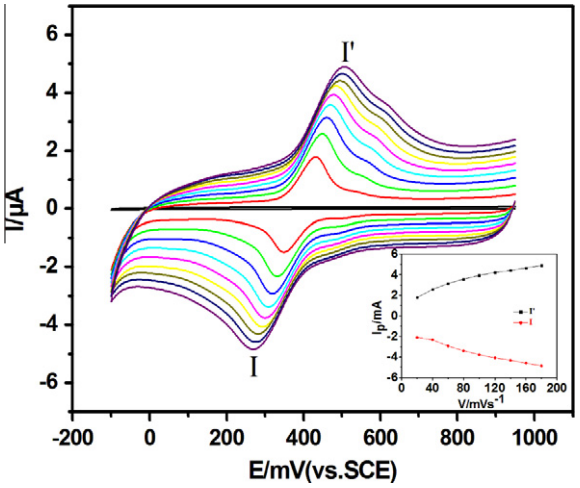

Fig. 10. Cyclic voltammograms of the **4**-CPE in 1 M H_2SO_4 aqueous solution at different scan rates (from inner to outer: the bare CPE, 20, 40, 60, 80, 100, 120, 140,160, 180 mV s^{-1}). The inset shows the plots of the anodic and cathodic peak currents against scan rates.

and common organic solvents. The title complexes are insoluble in the 1 M H_2SO_4 aqueous solution, so the electrochemical measurements of **1**-, **2**-, **3**- and **4**-CPE are carried out in it. In the potential range of +950 to 0 mV, there is no redox peak at the bare CPE. A reversible redox peak is observed at the **1**-, **2**-, **3**- and **4**-CPE, respectively, which can be attributed to the redox of Co(III)/Co(II) [38]. The mean peak potentials $E_{1/2} = (E_{pa} + E_{pc})/2$ are approximately 387 mV for **1**-CPE, 387 mV for **2**-CPE, 412 mV for **3**-CPE and 388 mV for **4**-CPE with the scan rate of 100 mV s^{-1}, respectively.

The effect of scan rates on the electrochemical behaviors of the **1**-, **2**-, **3**- and **4**-CPE are also reported in Figs. 9, 10 and S5, S6. With the scan rates increasing from 40 to 400 mV s^{-1} for **1**-CPE, 20 to 500 mV s^{-1} for **2**-CPE, 40 to 400 mV s^{-1} for **3**-CPE, 20 to 180 mV s^{-1} for **4**-**CPE**, the peak potentials changed gradually: the cathodic peak potentials gradually shift toward the negative direction and the corresponding anodic peak potentials shift toward the positive direction. The inset of Figs. 9, 10 and S5, S6 show that the anodic and cathodic peak currents are proportional to the scan rates, which suggest that the redox processes for **1**-, **2**-, **3**- and **4**-CPE are surface-controlled [39].

4. Conclusion

In conclusion, by introducing bix, dmpbbbm and aromatic monocarboxylic acids as mixed ligands, four Co(II) complexes have been successfully synthesized. Complexes **1**–**4** show diverse crystal architectures from dinuclear unit to 1D chain, which are ultimately extended into 1D to 3D supramolecular networks via π–π stacking interactions or H-bonding interactions. Our study demonstrates that the conformation and substitute groups of ligands have a great influence on the architectures of complexes **1**–**4**. In addition, the semirigid ligands play an important role in the formation of 1D helix chain. Moreover, the fluorescent properties and the electrochemical behaviors demonstrate the potential applications of the title complexes in the fluorescent and electrochemical field.

Acknowledgments

This work was supported by the National Natural Science Foundation of China (No. 21171025), and the Natural Science Foundation of Liaoning Province (Nos. 201102003 and 2009402007).

Appendix A. Supplementary material

CCDC 882813, 882814, 882815 and 882816 contain the supplementary crystallographic data for complexes **1**–**4**. These data can be obtained free of charge from The Cambridge Crystallographic Data Centre via www.ccdc.cam.ac.uk/data_request/cif. Supplementary data associated with this article can be found, in the online version, at http://dx.doi.org/10.1016/j.ica.2012.09.033.

References

[1] C.Y. Xu, Q.Q. Guo, X.J. Wang, H.W. Hou, Y.T. Fan, Cryst. Growth Des. 11 (2011) 1869.
[2] A. Ramaswamy, M. Froeyen, P. Herdewijn, A. Ceulemans, J. Am. Chem. Soc. 132 (2010) 587.
[3] J. Zhao, L. Mi, J. Hu, H. Hou, Y. Fan, J. Am. Chem. Soc. 130 (2008) 15222.
[4] S. Akine, H. Nagumo, T. Nabeshima, Inorg. Chem. 51 (2012) 5506.
[5] B.H. Ye, M.L. Tong, X.M. Chen, Coord. Chem. Rev. 249 (2005) 545.
[6] Y. Qi, F. Luo, S.R. Batten, Y.X. Che, J.M. Zheng, Cryst. Growth Des. 8 (2008) 2806.
[7] T.J. Burchell, D.J. Eisler, R.J. Puddephatt, Inorg. Chem. 43 (2004) 5550.
[8] G.C. Liu, S. Yang, X.L. Wang, Y.F. Wang, H.Y. Lin, J.X. Zhang, Zh. Neorg. Khim. (Russ. J. Inorg. Chem.) 12 (2011) 1918.
[9] J.Q. Chen, Y.P. Cai, H.C. Fang, Z.Y. Zhou, X.L. Zhan, G. Zhao, Z. Zhang, Cryst. Growth Des. 9 (2009) 1605.
[10] Y. Zhao, M.F. Lv, J. Fan, L. Luo, Z. Su, W.Y. Sun, Inorg. Chim. Acta 377 (2011) 138.
[11] Y.Y. Liu, Y.Y. Jiang, J. Yang, Y.Y. Liu, J.F. Ma, CrystEngComm 13 (2011) 6118.
[12] W.L. Zhou, W.Q. Li, G.H. Jin, D. Zhao, X.Q. Zhu, X.R. Meng, H.W. Hou, J. Mol. Struct. 995 (2011) 148.
[13] H. Zhong, H.L. Xie, S.H. Duan, Russ. J. Coord. Chem. 5 (2009) 30.
[14] W.Q. Kan, J.F. Ma, Y.Y. Liu, J. Yang, CrystEngComm 14 (2012) 2316.
[15] X.L. Wang, J.X. Zhang, G.C. Liu, H.Y. Lin, Y.Q. Chen, Z.H. Kang, Inorg. Chim. Acta 368 (2011) 207.
[16] X.L. Wang, L.L. Hou, J.W. Zhang, J.X. Zhang, G.C. Liu, S. Yang, CrystEngComm 14 (2012) 3936.
[17] X.L. Wang, S. Yang, G.C. Liu, J.X. Zhan, H.Y. Lin, A.X. Tian, Inorg. Chim. Acta 375 (2011) 70.
[18] X.L. Wang, S. Yang, G.C. Liu, L.L. Hou, H.Y. Lin, A.X. Tian, Transition Met. Chem. 36 (2011) 891.
[19] A.R. Xiao, Y.G. Li, E.B. Wang, L.L. Fan, H.Y. An, Z.M. Su, X. Lin, Inorg. Chem. 46 (2007) 4158.
[20] C.B. Aakeröy, J. Desper, B. Leonard, J.F. Urbina, Cryst. Growth Des. 5 (2005) 3865.
[21] H.Y. Lin, X.L. Wang, H.L. Hu, B.K. Chen, G.C. Liu, Solid State Chem. 11 (2009) 643.
[22] X.L. Wang, Z.H. Kang, E.B. Wang, C.W. Hu, Mater. Lett. 56 (2002) 393.
[23] G. Sheldrick, Acta Crystallogr., Sect. A 64 (2008) 112.
[24] C.C. Ji, L. Qin, Y.Z. Li, Z.J. Guo, H.G. Zheng, Cryst. Growth Des. 11 (2011) 480.
[25] W.W. He, J. Yang, Y. Yang, Y.Y. Liu, J.F. Ma, Dalton Trans. 41 (2012) 9737.
[26] Z.Q. Qin, M.C. Jennings, R.J. Puddephatt, Chem. Eur. J. 8 (2002) 735.
[27] X.L. Tang, W. Dou, J.A. Zhou, G.L. Zhang, W.S. Liu, L.Z. Yang, Y.L. Shao, CrystEngComm 13 (2011) 2890.
[28] X. Meng, Y. Song, H. Hou, H. Han, B. Xiao, Y. Fan, Y. Zhu, Inorg. Chem. 43 (2004) 5478.
[29] Q. Zhang, J. Zhang, Q.Y. Yu, M. Pan, C.Y. Su, Cryst. Growth Des. 10 (2010) 4076.
[30] C.Y. Xu, L.K. Li, Y.P. Wang, Q.Q. Guo, X.J. Wang, H.W. Hou, Y.T. Fan, Cryst. Growth Des. 11 (2011) 4667.
[31] X.J. Gu, D.F. Xue, Cryst. Growth Des. 6 (2006) 2551.
[32] L.J. Bellamy, The Infrared Spectra of Complex Molecules, Wiley, New York, 1958.
[33] H.N. Wang, X. Meng, C. Qin, X.L. Wang, G.S. Yang, Z.M. Su, Dalton Trans. 41 (2012) 1047.
[34] G.P. Yang, Y.Y. Wang, P. Liu, A.Y. Fu, Y.N. Zhang, J.C. Jin, Q.Z. Shi, Cryst. Growth Des. 10 (2010) 1443.
[35] K.H. He, W.C. Song, Y.W. Li, Y.Q. Chen, X.H. Bu, Cryst. Growth Des. 12 (2012) 1064.
[36] V.W.W. Yam, K.K.W. Lo, Chem. Soc. Rev. 28 (1999) 323.
[37] V. Amendola, L. Fabbrizzi, F. Foti, M. Licchelli, C. Mangano, P. Pallavicini, A. Poggi, D. Sacchi, A. Taglietti, Coord. Chem. Rev. 250 (2006) 273.
[38] T.V. Mitkina, N.F. Zakharchuk, D.Y. Naumov, O.A. Gerasko, D. Fenske, V.P. Fedin, Inorg. Chem. 47 (2008) 6748.
[39] X.L. Wang, B. Mu, H.Y. Lin, G.C. Liu, J. Organomet. Chem. 696 (2011) 2313.